electronics

Article

# Indoor Positioning Method by CNN-LSTM of Continuous Received Signal Strength Indicator

**Jae-hyuk Yoon [1], Hee-jin Kim [1], Dong-seok Lee [2] and Soon-kak Kwon [1,*]**

[1] Department of Computer Software Engineering, Dong-eui University, Busan 47340, Republic of Korea; gu9062@naver.com (J.-h.Y.); ghn07096@naver.com (H.-j.K.)
[2] AI Grand ICT Research Center, Dong-eui University, Busan 47340, Republic of Korea; 14177@deu.ac.kr
* Correspondence: skkwon@deu.ac.kr; Tel.: +82-51-890-1727

**Abstract:** This paper proposes an indoor positioning method based on Bluetooth Low Energy signals by Convolution Neural Network-Long Short-Term Memory (CNN-LSTM). The proposed method determines a receiver location based on distances from adjacent transmitters. The CNN-LSTM model estimates the distance from each transmitter using continuous signal strengths. To train and validate the model, the signal strengths are collected in several locations within various indoor environments. The positioning technique is adaptively selected based on the highest signal strength to avoid the interfering problem due to an excessively strong signal. If the signal strength exceeds a certain threshold, the location is determined using the proximity technique, which utilizes only the strongest signal instead of triangulation. In the experimental results, the proposed method demonstrated an average error of about 2.90 m, which is 34.2% better than a triangulation-based positioning method that does not utilize neural networks.

**Keywords:** indoor positioning; distance estimation; CNN-LSTM; triangulation; Bluetooth Low Energy



**Citation:** Yoon, J.-h.; Kim, H.-j.; Lee, D.-s.; Kwon, S.-k. Indoor Positioning Method by CNN-LSTM of Continuous Received Signal Strength Indicator. *Electronics* **2024**, *13*, 4518. https://doi.org/10.3390/electronics13224518

Academic Editors: Youngok Kim and Zhou Biao

Received: 23 October 2024
Revised: 12 November 2024
Accepted: 16 November 2024
Published: 18 November 2024



## 1. Introduction

Accurate positioning technology is required to provide effective location-based services [1–5]. For outdoor environments, the Global Positioning System (GPS) [6] enables precise positioning. However, GPS is difficult to use in indoor positioning systems (IPS) since GPS signals have limited ability to penetrate building structures such as concrete. IPS uses ultra-wideband [7,8], Wi-Fi, and Bluetooth signals as alternatives to GPS. These signals enable easy IPS deployment.

Wireless signal-based positioning primarily relies on signal path-loss or fingerprinting. While it can also utilize differences in the phase, angle, or time of arrival [9,10], these approaches are challenging to implement and have significant environmental limitations. Positioning techniques based on signal path-loss rely on the principle that signal strength is inversely proportional to the square of the distance between a transmitter and a receiver. However, this principle often does not apply well to actual indoor environments due to penetration loss and multi-path interference (MPI): penetration loss refers to the weakening of wireless signals caused by obstructions like building walls, and MPI occurs when interference arises between a signal received through a direct path and signals reflected off building structures. The log-distance path-loss model (LDPLM) [11] describes the relationship between the signal path distances and signal strength losses in indoor environments by introducing the parameter of the path-loss exponent for the degree of signal distortion caused by indoor structures. However, distance estimation using the LDPLM requires finding the optimal path-loss exponent for each indoor environment. Therefore, distance estimation using the LDPLM is difficult across various indoor environments. In addition, signal distortion may also occur due to interference between multiple signals from different transmitters. If the receiver is too close to a specific transmitter, the signal strengths from other transmitters become highly inaccurate. Consequently, an IPS based on signal path-loss becomes unreliable because of the signal distortions. To address these issues, indoor positioning often utilizes the fingerprinting technique [12–20]. Fingerprinting-based positioning determines the location by matching the received signal strengths to pre-collected data. The fingerprinting technique improves indoor positioning performance by collecting and utilizing the signal strength distortions caused by indoor environments in advance. However, this technique has a limitation in that it cannot be applied in areas where signals have not been collected in advance or where the environment has changed since the signals were collected.

The aim of this paper is to develop a low-cost, accurate IPS that can be used in various spaces with minimal signal data collection. In other words, the proposed IPS should be able to accurately determine the location even in areas where data have not been collected in advance. To achieve this, we utilize trilateration-based positioning, which determines the location using known transmitter positions and measured distances rather than relying on the fingerprinting technique commonly used for indoor positioning. Our previous study [21] proposed an indoor positioning method based on trilateration using Bluetooth Low Energy (BLE). This study estimates the distances from three adjacent transmitters using the LDPLM. Trilateration is applied by default for determining the location. However, if one of the measured distances to the receiver is too close, the location is determined using the proximity technique [22–26], which relies on only the single strongest signal as other signals are deemed unreliable due to signal interference. Nonetheless, previous studies did not fully resolve the limitations of indoor positioning in terms of distance estimation. In order to improve trilateration-based positioning, we estimate distances from the transmitters using a neural network that utilizes continuous signal strengths rather than a single or representative strength, as in traditional estimation methods. Continuous data, also known as time-series data, can be handled by Recurrent Neural Networks (RNNs), which have a recursive structure that carries the state from the previous stage into the current stage. Additionally, a 1D Convolutional Neural Network (CNN) with one-dimensional kernels can also process continuous data by detecting local patterns within the kernel size. A CNN-LSTM can process continuous signal data [27–30] by combining a 1D CNN with the LSTM [31], a type of RNN. In the CNN-LSTM, the CNN layers detect local features in the data, while the LSTM layers extract sequential features from these continuous local features. We adopt the CNN-LSTM to extract distance-related features from continuous signal strengths for distance estimation.

In this paper, we propose an indoor positioning method through a CNN-LSTM model using the continuous received signal strength indicators (RSSIs) of BLE signals. The CNN-LSTM model is trained using a dataset of RSSIs and corresponding distances collected from indoor environments, both with line of sight (LOS) and non-line of sight (NLOS) between the transmitter and receiver. The three distances from the adjacent transmitters are estimated by a CNN-LSTM model after a certain number of BLE RSSIs have been collected for each transmitter. The receiver location is determined by trilateration if all the distances are higher than a certain threshold; otherwise, the proximity technique is applied for indoor positioning.

The main contributions of this paper are as follows:

1. The proposed method improves on our previous study by introducing the CNN-LSTM model that uses continuous RSSIs to enhance robustness against signal distortions due to penetration loss and MPI;
2. In contrast to fingerprinting-based methods, the proposed approach enables indoor positioning across different areas, even in locations where signals have not been previously collected;
3. The proximity technique in the proposed method helps to preserve the positioning accuracy even if strong signals from a nearby transmitter significantly distort other signals.

The paper is structured as follows: Section 2 describes the related research; Section 3 presents the indoor positioning method through the CNN-LSTM model using continuous RSSIs; Section 4 shows the experimental results; and, finally, Section 5 provides the conclusions and future research directions.

## 2. Related Works

### 2.1. Log-Distance Path-Loss Model

The LDPLM [11] explains the path-loss of a wireless signal in indoor environments on a logarithmic scale. If the receiver and transmitter are separated by a distance $d$, the LDPLM estimates the RSSI as follows:

$$PL = PL_0 + 10n_p log_{10}(d/d_0), \tag{1}$$

where $PL_0$ is a reference RSSI measured at a known reference distance $d_0$ and $n_p$ is a path-loss exponent that describes the degree of signal distortion caused by indoor structures. Typically, $n_p$ is optimal at 2 or 3 in open indoor environments and between 4 and 6 in crowded environments. Rearranging (1) for $d$ is as follows:

$$d = 10^{\frac{PL-PL_0}{10n_p}} d_0. \tag{2}$$

The LDPLM can roughly estimate the distance from the transmitter based on the corresponding RSSI. However, the RSSI changes periodically due to MPI. In addition, the LDPLM is difficult to apply to various indoor environments. To overcome these LDPLM limitations, path-loss models based on neural networks are proposed. Ref. [32] shows that neural networks can replace the traditional path-loss models. Nguyen [33] proposes a path-loss prediction method for signals with multiple frequencies at once through a Deep Neural Network (DNN). However, it is still difficult to predict the path-loss in areas with complex spatial environments because the inputs to this network are only the distance, area type, and signal type. Wen [34] proposed a path-loss prediction model using an Artificial Neural Network (ANN) designed for aircraft IPS. This model takes the relative coordinates from transmitters and the signal type to predict the path-losses of multi-frequency signals in complex indoor environments. However, this method is difficult to apply across various spatial environments because it tends to overfit for a specific area. Elmezughi [35] improves path-loss prediction through an ensemble technique that combines the prediction results of ANN, 1D CNN, and LSTM layers. However, this study focuses on outdoor environments, so then it is difficult to apply in indoor environments. Studies on CNN-based path-loss models have been conducted to predict the path-loss from a given floor plan [36,37]. However, the path-loss models based on neural networks are hard to apply to untrained areas.

### 2.2. Positioning by Trilateration

A given location can be determined through geometric calculations using the coordinates of three points and their respective distances from that location. Trilateration is a positioning method based on this principle. GPS positioning is a prime example of its application. With the coordinates of three points ($x_k$, $y_k$) and their respective distances $d_k$ ($k$ = 1, 2, 3), the following equation holds:

$$\begin{aligned} d_1 &= \sqrt{(X - x_1)^2 + (Y - y_1)^2} \\ d_2 &= \sqrt{(X - x_2)^2 + (Y - y_2)^2} \\ d_3 &= \sqrt{(X - x_3)^2 + (Y - y_3)^2}, \end{aligned} \tag{3}$$

where ($X$, $Y$) are the coordinates of a given point. Rearranging (3) for ($X$, $Y$) is as follows:

$$\begin{aligned} X &= \frac{\left(d_2{}^2 - d_3{}^2 - x_2{}^2 + x_3{}^2 - y_2{}^2 + y_3{}^2\right)(y_2 - y_1) - (y_3 - y_2)\left(d_1{}^2 - d_2{}^2 - x_1{}^2 + x_2{}^2 - y_1{}^2 + y_2{}^2\right)}{2((y_2 - y_1)(x_3 - x_2) - (y_3 - y_2)(x_2 - x_1))} \\ Y &= \frac{\left(d_2{}^2 - d_3{}^2 - x_2{}^2 + x_3{}^2 - y_2{}^2 + y_3{}^2\right)(x_2 - x_1) - (x_3 - x_2)\left(d_1{}^2 - d_2{}^2 - x_1{}^2 + x_2{}^2 - y_1{}^2 + y_2{}^2\right)}{2((x_2 - x_1)(y_3 - y_2) - (x_3 - x_2)(y_2 - y_1))}. \end{aligned} \tag{4}$$

### 2.3. Indoor Positioning Methods Using Wireless Signals

Indoor positioning using wireless signals is classified into distance-based and fingerprinting-based methods. Trilateration is a common positioning technique for distance-based methods. The trilateration-based positioning methods can determine the receiver location through a simple geometrical calculation. However, the trilateration-based methods have the limitation that the path-loss model for the distance estimation is vulnerable to signal distortion. To address this limitation, signal correction methods are proposed for trilateration-based positioning. Fu [38] detected outliers through the Thompson Tau test for correcting the received signals. Ozer [39] applied a Kalman filter to the signal correction for real-time positioning. Jianyong [40] found a representative RSSI by calculating the weighted average of continuous RSSIs within a window of a certain size. Bai [41] introduced a Kalman filter and path-loss model fitting to reduce the noise in the received signals. Additionally, several studies [42,43] were conducted to improve trilateration-based positioning by optimizing the path-loss models. Trilateration is difficult to apply in areas where it is hard to receive at least three reliable signals. In such cases, the proximity technique can be utilized for positioning [22–26]. The proximity technique determines the receiver location based on the transmitter location generating this signal. Our previous study [21] proposes an indoor positioning method using both trilateration and the proximity technique. Normally, triangulation is used, but the proximity technique is applied if one distance is estimated to be too close. The existing distance-based methods are hard to apply across various spatial environments because the distance estimation models tend to be biased toward a specific indoor environment. In particular, it is difficult to design a distance estimation model that is applicable to various areas because the path-loss varies depending on indoor factors such as the area density.

Fingerprint-based positioning is more easily applicable to IPS because it collects signal information, including distortions, from multiple locations in advance. The location is determined by matching one or more indicators, such as RSSI or signal distortion metrics, which are the Channel State Information (CSI), the Reference Signal Received Power (RSRP), the Reference Signal Received Quality (RSRQ), or the Signal to Interference plus Noise Ratio (SINR), with the pre-corrected data. Recently, several studies have been conducted to improve indoor positioning using neural networks. The methods based on neural networks approach positioning as a classification task to predefined locations. Deep Neural Networks (DNN) were proposed to predict the receiver location through CSI [12] or RSSI [13]. CNN-based positioning methods [14–18] predict the location by matching an image generated from the received signal strengths with the stored fingerprint images. Wang [19] identifies candidates through CNN-based positioning and determines the location by verifying these candidates through the LDPLM. Hoang [20] predicts a route for the positioning through RNN using continuous RSSIs. However, these methods can be applied to only specific areas where the signal reception information is pre-collected.

Table 1 presents recent studies on indoor positioning methods using wireless signals. Neural networks have been applied to fingerprinting techniques. In contrast, research on distance-based methods that utilize neural networks is sparse.

**Table 1.** Recent indoor positioning studies using wireless signals.

| Study | Positioning Technique | Signal Type | Architecture |
|---|---|---|---|
| Song et al. [16] | Fingerprinting | Wi-Fi | Stacked autoencoder with 1D-CNN |
| Mazlan et al. [18] | Fingerprinting | BLE | CNN |
| Wang et al. [19] | Fingerprinting | 5G signal | CNN |
| Hoang et al. [20] | Fingerprinting | Wi-Fi | RNNs |
| Yoon et al. [21] | Trilateration | BLE | Kalman filter, moving window filter |
| Liu et al. [42] | Trilateration | WSN | Firefly algorithm, particle swarm optimization |
| Yang et al. [43] | Trilateration | Wi-Fi | Gaussian filter, linear regression |
| Bai et al. [41] | Fingerprinting, Trilateration | BLE | Kalman filter, machine learning (Naive Bayes, support-vector machines, random forests, BayesNet, J48 classification) |

## 3. Indoor Positioning Method Through CNN-LSTM of Continuous RSSIs

This paper proposes an indoor positioning method using continuous RSSIs received from several BLE transmitters. The proposed method adopts trilateration rather than the fingerprinting technique for indoor positioning in order to enable applicability to several areas. To address inaccurate distance estimation due to signal strength distortions caused by penetration loss and MPI, continuous BLE RSSIs are utilized to estimate distances through a CNN-LSTM model.

After collecting $N_r$ consecutive RSSIs for each of the three adjacent transmitters, the distances from each transmitter are estimated through the CNN-LSTM model. The closest among the estimated distances is used as the criterion for proximity. The location is determined by trilateration if the closest distance is larger than a certain threshold; otherwise, the proximity technique is applied to the positioning. Figure 1 shows the flow of the proposed method.

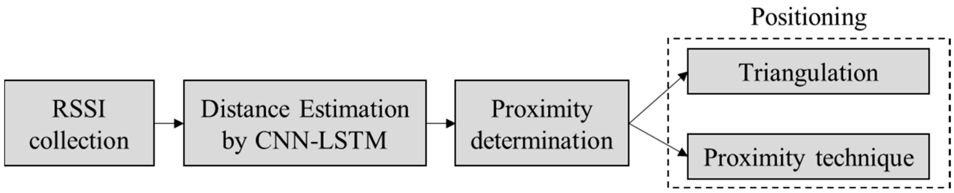


**Figure 1.** Flow of the proposed indoor positioning.

The indoor positioning in the proposed method consists of a receiver, BLE transmitters, and a server. The transmitters send their unique values of themselves, Media Access Control (MAC) addresses, to the receiver via their signals with a period of 100 ms. The receiver measures the RSSIs from the received BLE signals with a period of 100 ms and stores these with the received MAC address. Then, the stored data is sent to the server via wireless communication such as Wi-Fi. The server estimates the receiver location through the CNN-LSTM model from the continuously received RSSIs and provides location-based services. In this paper, the transmitter and the receiver are Feasycom FSC-BP101E [44]. We adopt Infineon CYW43439 [45], which is a module mounted on Raspberry Pi Pico W for wireless communications for Bluetooth and Wi-Fi, as the receiver. Tables 2 and 3 show the specifications of the transmitter and the receiver, respectively. Figure 2 shows the structure of the IPS.

**Table 2.** Transmitter device specifications.

| | |
|---|---|
| Device | FSC-BP101E |
| Manufacturer | Feasycom (Shenzhen, China) |
| Bluetooth version | 5.2 |
| Maximum transmit power | 5 dBm |
| Broadcast interval | 100 ms |

**Table 3.** Receiver device specifications.

| | |
|---|---|
| Device | Raspberry Pi Pico W |
| Manufacturer | Raspberry Pi Ltd. (Pencoed, UK) |
| Wireless communication module | Infineon CYW43439 |
| Bluetooth version | 5.2 |
| Minimum receiving interval | 7.5 ms |
| Minimum sensitivity for BLE signals | −94 dBm |

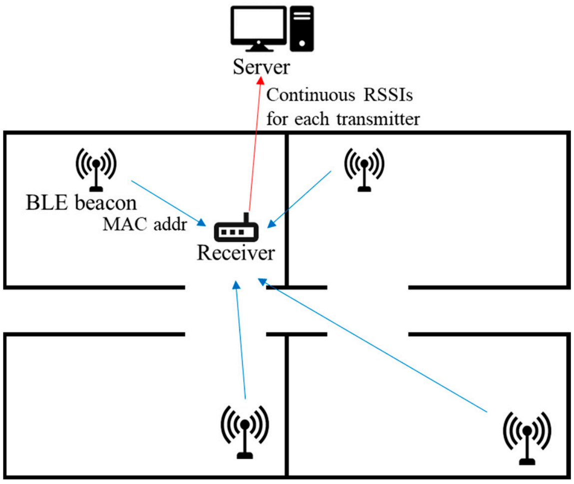


**Figure 2.** Structure of the proposed IPS.

### 3.1. Data Collection and Analysis

We collect data for the BLE signals from various areas. RSSIs from continuous BLE signals are collected from both LOS (line of sight) environments, where the direct path between the transmitter and receiver is open, and NLOS (non-line of sight) environments, where obstacles are present along the path. Figure 3 shows the indoor environments for the data collection in both LOS and NLOS environments. The devices used to collect the signals can reliably receive them within a distance of approximately 20 m in NLOS environments. Therefore, the signals are collected with the distance between the transmitter and receiver measured in 1 m increments, ranging from 1 m to 15 m. In this paper, continuous RSSIs were collected at varying distances across four different areas within each environment. During each collection, 1000 continuous RSSIs were gathered. In total, 120 collections were performed, yielding 120,000 RSSI measurements. Then, the continuous RSSIs gathered in 70% of the collections were used for model training, while the remaining 30% were used for model validation.

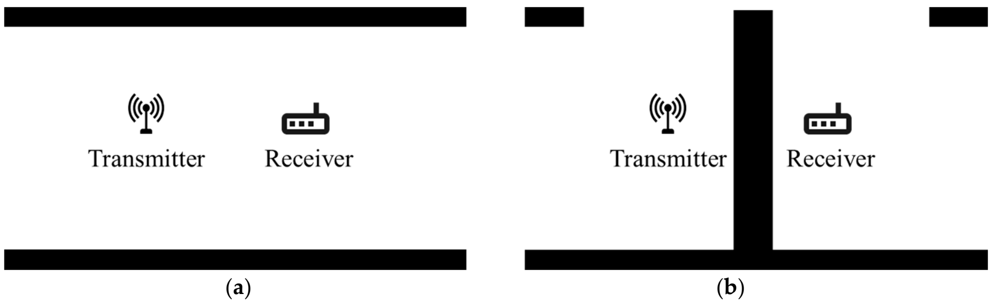


**Figure 3.** Indoor environments for the data collection: (**a**) LOS; (**b**) NLOS.

Figure 4 shows the average RSSIs for each distance in both LOS and NLOS environments. The RSSIs in the NLOS environment were attenuated by an average of 9.46 dBm compared to the LOS environment due to penetration loss. This suggests that traditional distance estimation by LDPLM may be accurate in either LOS or NLOS environments but not in both.

Figure 5 shows 100 continuous RSSIs for distances of 5 m and 10 m in both LOS and NLOS environments. The solid and dashed lines are measured RSSIs and the averages of these, respectively. The continuous RSSIs display waveforms with periodic fluctuations due to MPI. In other words, the periodic amplification and attenuation of signals occur due to phase differences between signals received from multiple paths. Additionally, temporary signal noise further distorts the received signals. These distortions make it difficult to estimate distances based on a single RSSI. However, robust distance estimation can be achieved by detecting common variation patterns based on distance.

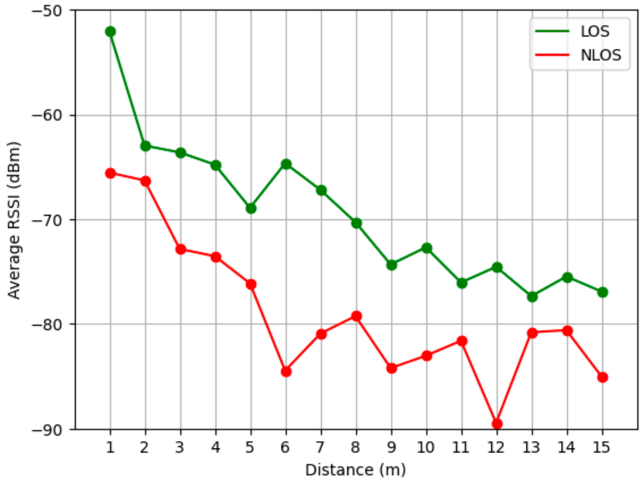


**Figure 4.** Comparison of RSSIs by distance between LOS and NLOS.

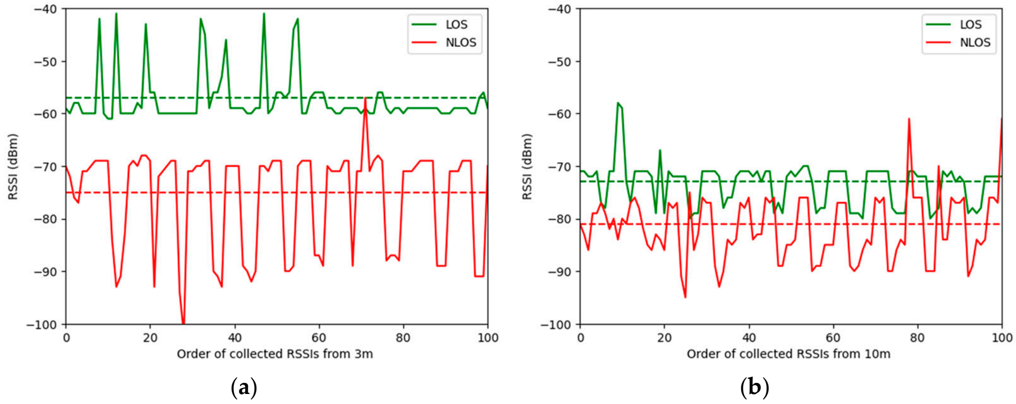


**Figure 5.** Continuous RSSIs for distances: (**a**) 3 m; (**b**) 5 m.

*3.2. CNN-LSTM Model for Distance Estimation*

A CNN-LSTM model is proposed for estimating the distance between the transmitter and receiver using continuous RSSIs. The proposed CNN-LSTM model consists of a CNN layer for extracting local features from the RSSIs, an LSTM layer for identifying sequential features, and a fully connected (FC) layer for estimating the distance. The CNN layer extracts $f_{cnn}$ local features through 1D convolution operations using 1D kernels with $l_k$ lengths from the continuous $N_r$ RSSIs. Afterwards, sequential features are identified from the local features using LSTMs stacked in $n_l$ layers. An LSTM unit maintains two states: a hidden state that represents the features at the current time step and a cell state, also known as long-term memory, which stores important inputs up to the current time step. In the stacked LSTMs, the input to each unit is the hidden state from the previous layer at the same time step. The FC layer estimates the distance between the transmitter and the receiver through regression using two linear transformations that output a vector of length $l_{fc}$ and a scalar value, respectively. The input to the FC layer is the final hidden state with $l_h$ lengths from the last LSTM layer. The Rectified Linear Unit (ReLU) is adopted as the activation function for both the CNN layer and the FC layer to introduce non-linearity and add sparsity to their outputs. However, the activation function is not applied to the final output of the FC layer. Figure 6 shows the network structure diagram of the proposed CNN-LSTM model.

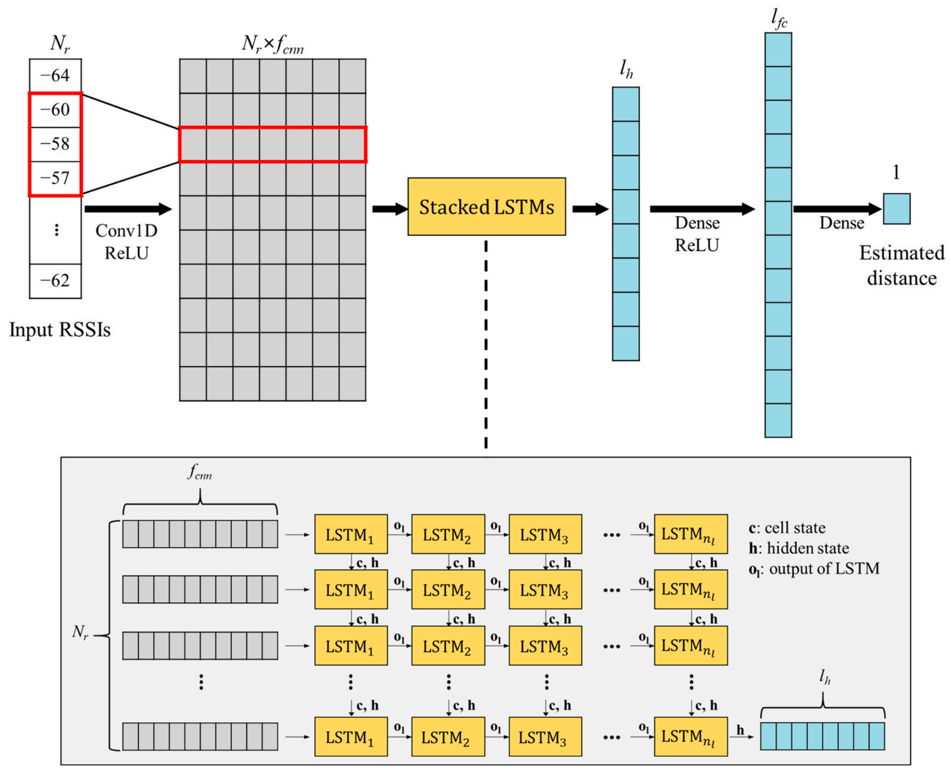


**Figure 6.** Network structures of the proposed CNN-LSTM model for distance estimation.

We generate a dataset to train and validate the proposed CNN-LSTM model by applying sliding windows with $N_r$ lengths to the collected RSSIs from the various areas, as shown in Figure 7. For model training, the loss function uses the Mean Squared Error (MSE), which is commonly applied in regression models.

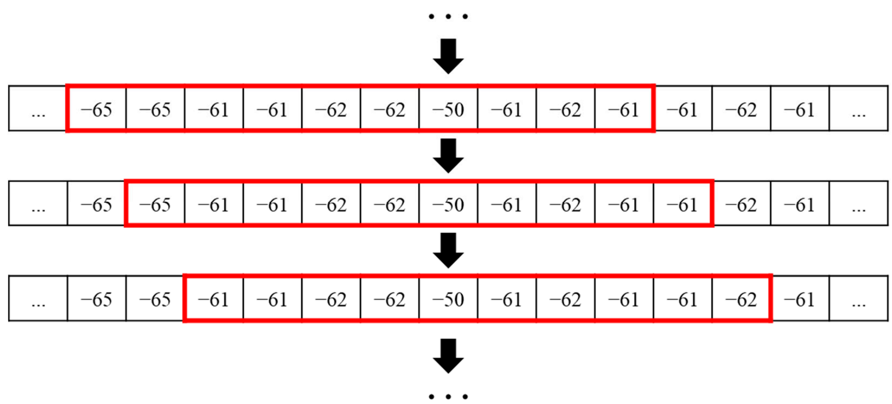

**Figure 7.** Sliding window of continuous RSSIs to generate dataset for training and validating.

### 3.3. Positioning Based on Distances

The receiver collects the continuous signals from each transmitter with known locations and measures the RSSIs. After $N_r$ RSSIs are collected from each of the three nearby transmitters, the distances from these transmitters are estimated through the CNN-LSTM model. To address the inaccurate distance estimation caused by the transmitter that is too close, we apply positioning based on the proximity technique, which is based on only one signal, from our previous study [21]. Proximity for the transmitter is determined based on the closest of the estimated distances. If the distance is larger than a certain threshold $T_p$, the location is determined by (4) for trilateration; otherwise, the proximity technique is applied. The traditional proximity technique determines the location as the reference transmitter with the strongest received signal, which leads to low accuracy. To improve the positioning accuracy, the estimated location is compensated based on the locations of the adjacent transmitters. For the modified proximity technique, a distance $d$ is estimated based on the RSSIs from the reference transmitter. The location is determined at a point that is $d$ distance away from the reference transmitter in the direction bisecting the angle formed by the two adjacent transmitters. When the transmitters are arranged in two rows, as shown in Figure 8, the location is determined by the following equation:

$$\begin{aligned} X &= x_0 + d_0 \tfrac{x_1+x_2-2x_0}{|v_1+v_2|} \\ Y &= y_0 + d_0 \tfrac{y_1+y_2-2y_0}{|v_1+v_2|}, \end{aligned} \tag{5}$$

where $(x_0, y_0)$ and $(x_k, y_k)$ ($k$ = 1, 2) are the coordinates of the reference transmitter and the two adjacent transmitters, respectively; $d_0$ is an estimated distance corresponding to the signal from the reference transmitter; and $v_1$ and $v_2$ are two vectors generated from the coordinates of the reference transmitter and each adjacent transmitter, as follows:

$$\begin{aligned} v_1 &= (x_1 - x_0, y_1 - y_0) \\ v_2 &= (x_2 - x_0, y_2 - y_0) \\ |v_1 + v_2| &= \sqrt{(x_1 + x_2 - 2x_0)^2 + (y_1 + y_2 - 2y_0)^2}. \end{aligned} \tag{6}$$

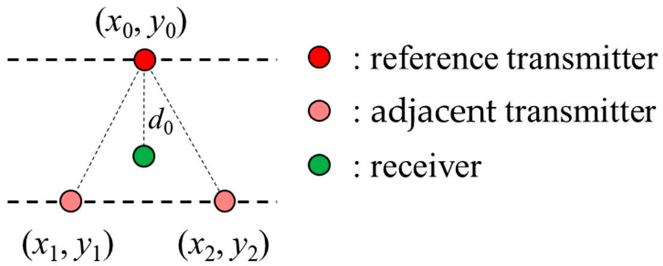


**Figure 8.** Positioning through the modified proximity technique.

## 4. Experimental Results and Discussion

We conducted experiments to measure the indoor positioning performance of the proposed method. For the experiments, the initial parameters for the CNN-LSTM model were as follows: the numbers of CNN layers and LSTM layers were 1 and 5, respectively; the kernel size $k$ and the number of output features $f_{cnn}$ in the CNN layer were 3 and 32, respectively; the length $l_h$ of the hidden state for the LSTM units was 64; and the length $l_{fc}$ of the first output of the FC layer was 128. The input size $N_r$ for the CNN-LSTM model was 10. During model training, the initial learning rate and the number of epochs were set to $10^{-4}$ and 6000, respectively. In the experiment, we collected RSSIs in four different areas under both LOS and NLOS environments, following the same data collection process used for model training and validation. During each collection, 600 continuous RSSIs were gathered. We measured the Mean Squared Errors (MSEs), the Mean Absolute Errors (MAEs), the Root Mean Squared Errors (RMSEs), and the coefficients of determination (R-squared, $R^2$) as metrics to evaluate the distance estimation model. These metrics were calculated as follows:

$$\begin{aligned} \mathrm{MSE} &= \frac{1}{N}\sum_{i=1}^{N}(t_i - o_i)^2 \\ \mathrm{MAE} &= \frac{1}{N}\sum_{i=1}^{N}|t_i - o_i|^2 \\ \mathrm{RMSE} &= \sqrt{\mathrm{MSE}} \\ \mathrm{R}^2 &= 1 - \left(\sum_{i=1}^{N}(t_i - o_i)^2 / \sum_{i=1}^{N}(t_i - \bar{t})^2\right), \end{aligned} \tag{7}$$

where $N$ is the number of samples for the experiment, $t_i$ and $o_i$ are the actual distance and the estimated distance for the $i$-th input data, respectively, and $\bar{t}$ is the average actual distance.

We compared the performance of our method with that of traditional LDPLMs. For the LDPLMs, $d_0$ and $PL_0$ in (2) are 1 and $-44$, respectively. The path-loss exponent $n_p$ in (2) is determined based on the density of the indoor environment. This parameter is optimal at higher values in densely packed indoor environments, where signal penetration and reflection are more frequent. We confirmed that the optimal $n_p$ is 3.88 when considering all indoor environments. Therefore, we measured the estimation performances for three LDPLMs with $n_p$ of 3, 4, and 3.88, respectively, in both LOS and NLOS. In LDPLMs, the distances are estimated through (2) from the average of 10 continuous RSSIs.

Table 4 and Figure 9 show a comparison of distance estimation between the proposed method and the LDPLMs. The proposed method outperforms both LDPLMs in all metrics. For the LDPLMs, the estimation distances tend to decrease as $n_p$ increases. Therefore, the LDPLM with higher $n_p$ is more accurate in the NLOS environments where the path-loss is larger, as shown in Figure 4. Conversely, the LDPLM performance in LOS environments improves with lower $n_p$. Interestingly, the LDPLM with the optimal $n_p$ exhibits a lower average estimation error than the other LDPLMs, but it is not the best LDPLM in every individual environment. The proposed CNN-LSTM model improves the RMSE of distance estimation for all environments by an average of about 73%. While the specific LDPLM achieves accurate measurements in one indoor environment, its performance drops significantly in another. This suggests that the LDPLM is not well-suited to distance estimation across diverse indoor environments. In contrast, the proposed method demonstrates strong performance in various indoor environments.

**Table 4.** Comparison of distance estimation performance between the proposed method and LDPLMs in LOS and NLOS.

| Model | Indoor Environment | MAE (m) | MSE ($m^2$) | RMSE (m) | $R^2$ |
|---|---|---|---|---|---|
| LDPLM ($n_p$ = 3) | LOS | 1.9640 | 6.3460 | 2.5191 | 0.6607 |
| | NLOS | 8.1787 | 119.4551 | 10.9296 | 0.5479 |
| | ALL | 5.0713 | 62.9006 | 7.9310 | 0.5554 |
| LDPLM ($n_p$ = 3.88) | LOS | 3.3354 | 17.1855 | 4.1456 | 0.4033 |
| | NLOS | 2.9308 | 13.7006 | 3.7014 | 0.5238 |
| | ALL | 3.1330 | 15.4431 | 3.9298 | 0.4635 |
| LDPLM ($n_p$ = 4) | LOS | 3.7063 | 21.1582 | 4.5998 | 0.3983 |
| | NLOS | 2.7112 | 11.8825 | 3.4471 | 0.4706 |
| | ALL | 3.2087 | 16.5203 | 4.0645 | 0.4265 |
| Proposed | LOS | 0.6531 | 1.4222 | 1.1925 | 0.9265 |
| | NLOS | 0.3998 | 0.9208 | 0.9596 | 0.9516 |
| | ALL | 0.5264 | 1.1715 | 1.0823 | 0.9390 |

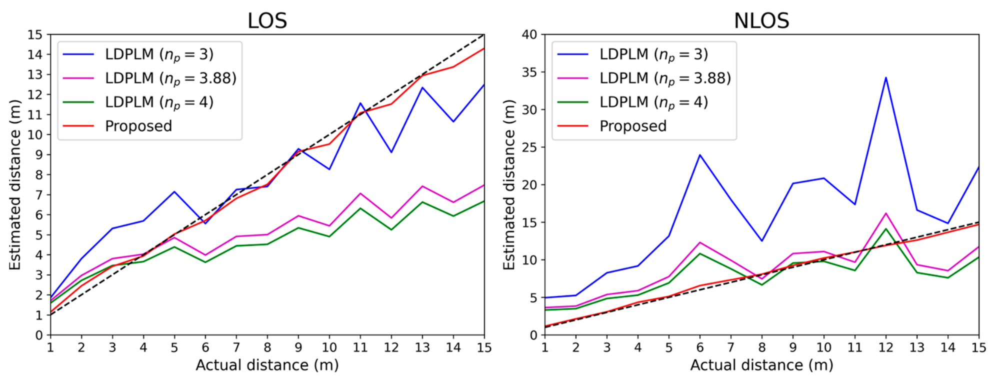


**Figure 9.** Distance estimation results for each distance.

Table 5 presents the results of the ablation study for the CNN-LSTM model. Even the model with only the CNN layer showed a significant performance improvement compared to the traditional LDPLMs, though not as substantial as the model with only the LSTM layer. The LSTM layer greatly enhanced the distance estimation over the traditional path-loss model. The model with both the CNN and LSTM layers slightly further improved the performance compared to the model with only the LSTM layer. This suggests that the CNN layer helps to refine the input data and reduce noise.

**Table 5.** Ablation study results for the CNN-LSTM model.

| Model Structure | MAE (m) | MSE ($m^2$) | RMSE (m) |
|---|---|---|---|
| Only CNN | 1.7363 | 5.1878 | 2.2777 |
| Only LSTM | 0.6338 | 1.4710 | 1.2128 |
| CNN + LSTM | 0.5264 | 1.1715 | 1.0823 |

Table 6 shows the performance based on the number of CNN and LSTM layers. The performance of the distance estimation improves as the number of LSTM layers increases. However, the performance decreases in models with six or more LSTM layers due to overfitting caused by excessive model complexity. The optimal number of CNN layers is one, as the performance declines in the models where the number of layers exceeds two.

**Table 6.** Distance estimation performances for structures of the CNN-LSTM model.

| No. CNN | No. LSTM | MAE (m) | MSE ($m^2$) | RMSE (m) |
|---|---|---|---|---|
| 1 | 1 | 1.3601 | 3.8873 | 1.9716 |
| | 2 | 0.9574 | 2.3922 | 1.5467 |
| | 3 | 0.7808 | 1.9673 | 1.4026 |
| | 4 | 0.6236 | 1.3831 | 1.1760 |
| | 5 | 0.5264 | 1.1715 | 1.0823 |
| | 6 | 0.5339 | 1.3458 | 1.1601 |
| 2 | 1 | 1.4984 | 4.6294 | 2.1516 |
| | 2 | 0.9865 | 2.5512 | 1.5972 |
| | 3 | 0.7404 | 1.8132 | 1.3466 |
| | 4 | 0.7186 | 1.8522 | 1.3610 |
| | 5 | 0.5748 | 1.3697 | 1.1703 |
| | 6 | 0.5271 | 1.3309 | 1.1536 |

Table 7 shows the performance comparison based on the activation functions. We compared the proposed models with ReLU and GELU as the activation functions. Although GELU is generally known to outperform ReLU, the results demonstrated that increasing the sparsity of the layer outputs by ReLU is more effective in the proposed method than increasing the learning efficiency by GELU.

**Table 7.** Distance estimation performance for the activation function for the CNN-LSTM model.

| Activate Function | MAE (m) | MSE ($m^2$) | RMSE (m) |
|---|---|---|---|
| ReLU | 0.5264 | 1.1715 | 1.0823 |
| GELU | 0.5827 | 1.4204 | 1.1918 |

We measured the accuracy of the indoor positioning for several locations. The indoor environment for the experiment is shown in Figure 10. The transmitters were arranged in two rows, with three adjacent transmitters forming an equilateral triangle with a side length of 15 m. The positioning was conducted for three types of locations: side, which included eight points located 1 m from the transmitters; center, which included six points at the center of the three adjacent transmitters; and others, which consisted of six arbitrarily selected points. The positioning error was measured as a Euclidean distance between the estimated coordinates and the actual coordinates. The threshold $T_p$ for the proximity determination was set to 2.

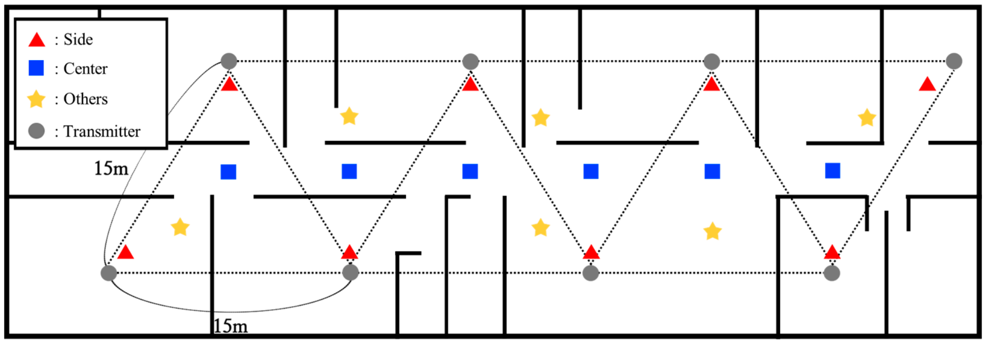


**Figure 10.** Indoor environment for indoor positioning experiment.

We compared the indoor positioning accuracy of the proposed method with that of our previous method [21]. The previous method enhances the distance estimations based on RSSIs by removing outliers and applying a Kalman filter. The position is determined using trilateration or the proximity technique. The estimated position is further refined through location outlier removal and a moving average filter. This previous method has been shown to achieve more accurate indoor positioning than traditional trilateration-based approaches.

Table 8 compares the positioning accuracies of the proposed method with those of our previous study and traditional trilateration-based positioning. The results indicate that the proposed method improves the positioning accuracy by approximately 35% compared to the previous study. The lowest accuracies are observed at the side points when the proximity technique is not applied. This demonstrates that excessive proximity to one transmitter causes significant distortion to the signals from other transmitters. This issue can be resolved by positioning based on a single, highly reliable RSSI, as shown in the results where the proximity technique is applied. By applying the proximity technique, the accuracy improves by approximately 44%.

**Table 8.** Comparisons of indoor positioning performances.

| **Positioning Method** | **MAE (m)** | | | |
|---|---|---|---|---|
| | **Side** | **Center** | **Others** | **Average** |
| Traditional trilateration | 9.41 | 6.28 | 8.05 | 8.06 |
| Previous study [21] | 3.16 | 2.87 | 7.63 | 4.41 |
| Proposed (no proximity technique) | 4.19 | 2.59 | 4.75 | 3.88 |
| Proposed (applying proximity technique) | 1.76 | 2.59 | 4.75 | 2.90 |

## 5. Conclusions

In this paper, we proposed an indoor positioning method by estimating the distances between the receiver and the transmitters through the CNN-LSTM model. To train and validate the CNN-LSTM model, continuous RSSIs were collected in both LOS and NLOS environments. After estimating the distances of the three adjacent transmitters, the positioning technique was adaptively selected from trilateration using the three estimated distances and the proximity technique, which used only the strongest signal. The experimental results showed that the proposed CNN-LSTM model improved the distance estimation accuracy by an average of about 73% compared to the traditional LDPLM. For indoor positioning, the proposed method outperformed our previous study by 34.2%. The proposed method enhances indoor positioning by introducing the CNN-LSTM model to estimate distances using consecutive RSSI measurements. Furthermore, it can be used for indoor positioning in areas where signals have not been previously collected, without the need for additional model training. Therefore, the proposed method can be applicable to developing affordable and easy-to-implement IPS. However, new signal collection and model retraining are required if there are changes in receive intervals. In future research, we plan to study a distance estimation method independent of interval variations using a model with a parallel layer structure that can capture distance-related features from continuous signals with various receive intervals.

**Author Contributions:** Conceptualization, J.-h.Y., H.-j.K., and S.-k.K.; software, J.-h.Y. and H.-j.K.; writing—original draft preparation, J.-h.Y., D.-s.L., and S.-k.K.; supervision, S.-k.K. All authors have read and agreed to the published version of the manuscript.

**Funding:** This research was partly supported by the Innovative Human Resource Development for Local Intellectualization program through the Institute of Information & Communications Technology Planning & Evaluation (IITP) grant funded by the Korean government (MSIT) (IITP-2024-RS-2020-II201791, 100%), by the BB21plus funded by Busan Metropolitan City and Busan Techno Park and by a Dong-Eui University Grant (202401420001).

**Institutional Review Board Statement:** Not applicable.

**Data Availability Statement:** The data are contained within the article.

**Conflicts of Interest:** The authors declare no conflicts of interest.

## References

1. Zaim, D.; Bellafkih, M. Bluetooth Low Energy (BLE) based geomarketing system. In Proceedings of the 2016 11th International Conference on Intelligent Systems: Theories and Applications (SITA), Mohammedia, Morocco, 19–20 October 2016; pp. 1–6.
2. Guerreiro, J.A.; Ahmetovic, D.; Sato, D.; Kitani, K.; Asakawa, C. Airport Accessibility and Navigation Assistance for People with Visual Impairments. In Proceedings of the Conference on Human Factors in Computing Systems, Glasgow, UK, 4–9 May 2019; pp. 1–14.
3. Hwangbo, H.; Kim, J.; Lee, Z.; Kim, S. Store Layout Optimization Using Indoor Positioning System. *Int. J. Distrib. Sens. Netw.* **2017**, *13*, 1550147717692585. [CrossRef]
4. Fadzilla, M.A.; Harun, A.; Shahriman, A.B. Localization Assessment for Asset Tracking Deployment by Comparing an Indoor Localization System with a Possible Outdoor Localization System. In Proceedings of the International Conference on Computational Approach in Smart Systems Design and Applications, Kuching, Malaysia, 15–17 September 2018; pp. 1–6.
5. Yang, Y.; Ding, Y.; Yuan, D.; Wang, G.; Xie, X.; Liu, Y.; He, T.; Zhang, D. TransLoc: Transparent Indoor Localization with Uncertain Human Participation for Instant Delivery. In Proceedings of the Annual International Conference on Mobile Computing and Networking, London, UK, 21–25 September 2020; pp. 1–14.
6. Parkinson, B.W. Introduction and Heritage of NAVSTAR, the Global Positioning System. In *Global Positioning System: Theory and Applications*, 1st ed.; Parkinson, B.W., Spilker, J.J., Eds.; American Institute of Aeronautics and Astronautics: Washington, DC, USA, 1996; Volume 1, pp. 3–28.
7. Yassin, A.; Nasser, Y.; Awad, M.; Al-Dubai, A.; Liu, R.; Yuen, C.; Raulefs, R.; Aboutanios, E. Recent Advances in Indoor Localization: A Survey on Theoretical Approaches and Applications. *IEEE Commun. Surv. Tutor.* **2017**, *19*, 1327–1346. [CrossRef]
8. Dong, J.; Lian, Z.; Xu, J.; Yue, Z. UWB localization based on improved robust adaptive cubature Kalman Filter. *Sensors* **2023**, *23*, 2669. [CrossRef] [PubMed]
9. Florio, A.; Avitabile, G.; Coviello, G. Digital Phase Estimation through an I/Q Approach for Angle of Arrival Full-Hardware Localization. In Proceedings of the IEEE Asia Pacific Conference on Circuits and Systems, Ha Long, Vietnam, 8–10 December 2020; pp. 106–109.
10. Zafari, F.; Gkelias, A.; Leung, K.K. A Survey of Indoor Localization Systems and Technologies. *IEEE Commun. Surv. Tutor.* **2019**, *21*, 2568–2599. [CrossRef]
11. Rappaport, T.S. *Wireless Communications: Principles and Practice*, 2nd ed.; Prentice Hall: Hoboken, NJ, USA, 2002; pp. 102–104.
12. Wang, X.; Gao, L.; Mao, S.; Pandey, S. CSI-Based Fingerprinting for Indoor Localization: A Deep Learning Approach. *IEEE Trans. Veh. Technol.* **2017**, *66*, 763–776. [CrossRef]
13. Lu, H.; Xingli, G.; Shuang, L.; Heng, Z.; Yaning, L.; Ruihui, Z. Indoor Positioning Technology Based on Deep Neural Networks. In Proceedings of the Ubiquitous Positioning, Indoor Navigation and Location-Based Services, Wuhan, China, 22–23 March 2018; pp. 1–6.
14. Chen, H.; Zhang, Y.; Li, W.; Tao, X.; Zhang, P. ConFi: Convolutional Neural Networks-Based Indoor Wi-Fi Localization Using Channel State Information. *IEEE Access* **2017**, *5*, 18066–18074. [CrossRef]

15. Jang, J.-W.; Hong, S.N. Indoor Localization with WiFi Fingerprinting Using Convolutional Neural Network. In Proceedings of the International Conference on Ubiquitous and Future Networks, Prague, Czech Republic, 3–6 July 2018; pp. 753–758.
16. Song, X.; Fan, X.; He, X.; Xiang, C.; Ye, Q.; Huang, X.; Fang, G.; Chen, L.L.; Qin, J.; Wang, Z. CNNLoc: Deep-Learning Based Indoor Localization with WiFi Fingerprinting. In Proceedings of the IEEE SmartWorld, Ubiquitous Intelligence and Computing, Advanced and Trusted Computing, Scalable Computing and Communications, Cloud and Big Data Computing, Internet of People and Smart City Innovation, Leicester, UK, 19–23 August 2019; pp. 589–595.
17. Mittal, A.; Tiku, S.; Pasricha, S. Adapting Convolutional Neural Networks for Indoor Localization with Smart Mobile Devices. In Proceedings of the Great Lakes Symposium on VLSI, Chicago, IL, USA, 23–25 May 2018; pp. 117–122.
18. Mazlan, A.B.; Ng, Y.H.; Tan, C.K. A Fast Indoor Positioning Using a Knowledge-Distilled Convolutional Neural Network (KD-CNN). *IEEE Access* **2022**, *10*, 65326–65338. [CrossRef]
19. Wang, Y.; Zhao, K.; Zheng, Z.; Ji, W.; Huang, S.; Ma, D. Indoor Positioning with CNN and Path-Loss Model Based on Multivariable Fingerprints in 5G Mobile Communication System. *Sensors* **2022**, *22*, 3179. [CrossRef]
20. Hoang, M.T.; Yuen, B.; Dong, X.; Lu, T.; Westendorp, R.; Reddy, K. Recurrent Neural Networks for Accurate RSSI Indoor Localization. *IEEE Internet Things J.* **2019**, *6*, 10639–10651. [CrossRef]
21. Yoon, J.H.; Kim, H.J.; Kwon, S.K. Proximity-Based Adaptive Indoor Positioning Method Using Received Signal Strength Indicator. *Appl. Sci.* **2024**, *14*, 3319. [CrossRef]
22. Sundaram, N.; Ramanathan, P. Connectivity-Based Location Estimation Scheme for Wireless ad hoc Networks. In Proceedings of the IEEE Global Telecommunications Conference, Taipei, Taiwan, 17–21 November 2002; pp. 143–147.
23. Doherty, L.; Pister, K.S.J.; Ghaoui, L.E. Convex Position Estimation in Wireless Sensor Networks. In Proceedings of the IEEE Infocom 2001, Anchorage, AK, USA, 22–26 April 2001; pp. 1655–1663.
24. Nagpal, R.; Shrobe, H.; Bachrach, J. Organizing a Global Coordinate System from Local Information on an Ad Hoc Sensor Network. In Proceedings of the International Workshop on Information Processing in Sensor Networks, Palo Alto, CA, USA, 22–23 April 2003.
25. Niculescu, D.; Nath, B. Ad hoc Positioning System. In Proceedings of the IEEE Global Telecommunications Conference, San Antonio, TX, USA, 25–29 November 2001; pp. 2926–2931.
26. Brida, P.; Matula, M.; Duha, J. Using Proximity Technology for Localization in Wireless Sensor Networks. *Commun. Sci. Lett. Univ. Zilina* **2007**, *9*, 50–54. [CrossRef]
27. Reddy, K.R.; Harsha Vardhan, P.N.; Pary, S.; Sharma, S.; Sanjay, M. A CNN-LSTM Model for Sleep Stage Scoring Using EEG Signals. In Proceedings of the International Conference on Communication, Circuits, and Systems, Bhubaneswar, India, 27–28 April 2023; pp. 1–6.
28. Islam, Z.; Abdel-Aty, M.; Mahmoud, N. Using CNN-LSTM to Predict Signal Phasing and Timing Aided by High-Resolution Detector Data. *Transp. Res. Part C Emerg. Technol.* **2022**, *141*, 103742. [CrossRef]
29. Parida, L.; Moharana, S.; Ferreira, V.M.; Giri, S.K.; Ascensão, G. A Novel CNN-LSTM Hybrid Model for Prediction of Electro-Mechanical Impedance Signal Based Bond Strength Monitoring. *Sensors* **2022**, *22*, 9920. [CrossRef]
30. Shang, L.; Zhang, Z.; Tang, F.; Cao, Q.; Pan, H.; Lin, Z. CNN-LSTM Hybrid Model to Promote Signal Processing of Ultrasonic Guided Lamb Waves for Damage Detection in Metallic Pipelines. *Sensors* **2023**, *23*, 7059. [CrossRef] [PubMed]
31. Hochreiter, S.; Schmidhuber, J. Long Short-term Memory. *Neural Comput.* **1997**, *9*, 1735–1780. [CrossRef] [PubMed]
32. Elmezughi, M.K.; Salih, O.; Afullo, T.J.; Duffy, K.J. Comparative Analysis of Major Machine-Learning-Based Path Loss Models for Enclosed Indoor Channels. *Sensors* **2022**, *22*, 4967. [CrossRef] [PubMed]
33. Nguyen, C.; Cheema, A.A. A Deep Neural Network-Based Multi-Frequency Path Loss Prediction Model from 0.8 GHz to 70 GHz. *Sensors* **2021**, *21*, 5100. [CrossRef]
34. Wen, J.; Zhang, Y.; Yang, G.; He, Z.; Zhang, W. Path Loss Prediction Based on Machine Learning Methods for Aircraft Cabin Environments. *IEEE Access* **2019**, *7*, 159251–159261. [CrossRef]
35. Elmezughi, M.K.; Salih, O.; Afullo, T.J.; Duffy, K.J. Path Loss Modeling Based on Neural Networks and Ensemble Method for Future Wireless Networks. *Heliyon* **2023**, *9*, e19685. [CrossRef]
36. Cheng, H.; Lee, H.; Ma, S. CNN-Based Indoor Path Loss Modeling with Reconstruction of Input Images. In Proceedings of the International Conference on Information and Communication Technology Convergence, Jeju, Republic of Korea, 17–19 October 2018; pp. 605–610.
37. Kuno, N.; Yamada, W.; Sasaki, M.; Takatori, Y. Convolutional Neural Network for Prediction Method of Path Loss Characteristics Considering Diffraction and Reflection in an Open-Square Environment. In Proceedings of the URSI Asia-Pacific Radio Science Conference, New Delhi, India, 9–15 March 2019; pp. 1–3.
38. Fu, Y.; Chen, P.; Yang, S.; Tang, J. An Indoor Localization Algorithm Based on Continuous Feature Scaling and Outlier Deleting. *IEEE Internet Things J.* **2018**, *5*, 1108–1115. [CrossRef]
39. Ozer, A.; John, E. Improving the Accuracy of Bluetooth Low Energy Indoor Positioning System Using Kalman Filtering. In Proceedings of the International Conference on Computational Science and Computational Intelligence, Las Vegas, NV, USA, 15–17 December 2016.
40. Jianyong, Z.; Haiyong, L.; Zili, C.; Zhaohui, L. RSSI Based Bluetooth Low Energy Indoor Positioning. In Proceedings of the International Conference on Indoor Positioning and Indoor Navigation, Busan, Republic of Korea, 27–30 October 2014; pp. 526–533.

41. Bai, L.; Ciravegna, F.; Bond, R.; Mulvenna, M. A Low-Cost Indoor Positioning System Using Bluetooth Low Energy. *IEEE Access* **2020**, *8*, 136858–136871. [CrossRef]
42. Liu, Y.; Li, N.; Wang, D.; Guan, T.; Wang, W.; Li, J.; Li, N. Optimization Algorithm of RSSI Transmission Model for Distance Error Correction. In Proceedings of the Advances in Intelligent Information Hiding and Multimedia Signal Processing, Jilin, China, 18–20 July 2020; Springer: Singapore, 2020; pp. 27–36.
43. Yang, J.; Deng, S.; Lin, M.; Xu, L. An Adaptive Calibration Algorithm Based on RSSI and LDPLM for Indoor Ranging and Positioning. *Sensors* **2022**, *22*, 5689. [CrossRef] [PubMed]
44. FSC-BP101E Datasheet. Available online: https://www.feasycom.com/datasheet/fsc-bp101e.pdf (accessed on 7 November 2024).
45. CYW43439 Datasheet. Available online: https://www.mouser.com/datasheet/2/196/Infineon_CYW43439_DataSheet_v03_00_EN-3074791.pdf (accessed on 7 November 2024).